Supplementary Information (SI) for New Journal of Chemistry.

Phase-effect of Bi_2O_3 in photocatalytic degradation of o-chlorophenol via a preferential dechlorination pathway

Xingyu Jin[a], Ying Wang[a], Limin Wang[a], Rui Yan[a,b]*, Ekateria Kozlova[c], Zhijun Li[a], Binhong Qu[a], Yang Qu[a]* and Liqiang Jing[a]

[a].Key Laboratory of Functional Inorganic Materials Chemistry (Heilongjiang University), Ministry of Education, School of Chemistry and Materials Science, International Joint Research Center for Catalytic Technology, Harbin 150080, P. R. China. E-mail:quyang@hlju.edu.cn

[b].Key Laboratory for Photonic and Electronic Bandgap Materials, Ministry of Education, College of Chemistry & Chemical Engineering, Harbin Normal University, Harbin, 150025, China.E-mail:yanrui-1981@163.com

[c].Federal Research Center, Boreskov Institute of Catalysis, 630090, Novosibirsk, Russia.

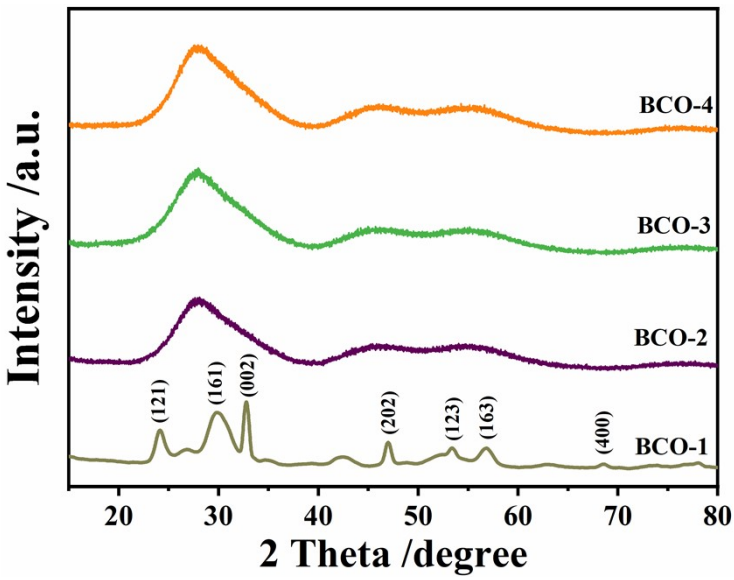

Figure S1. XRD patterns of different carbonates and bicarbonates treated CAU-17 samples.

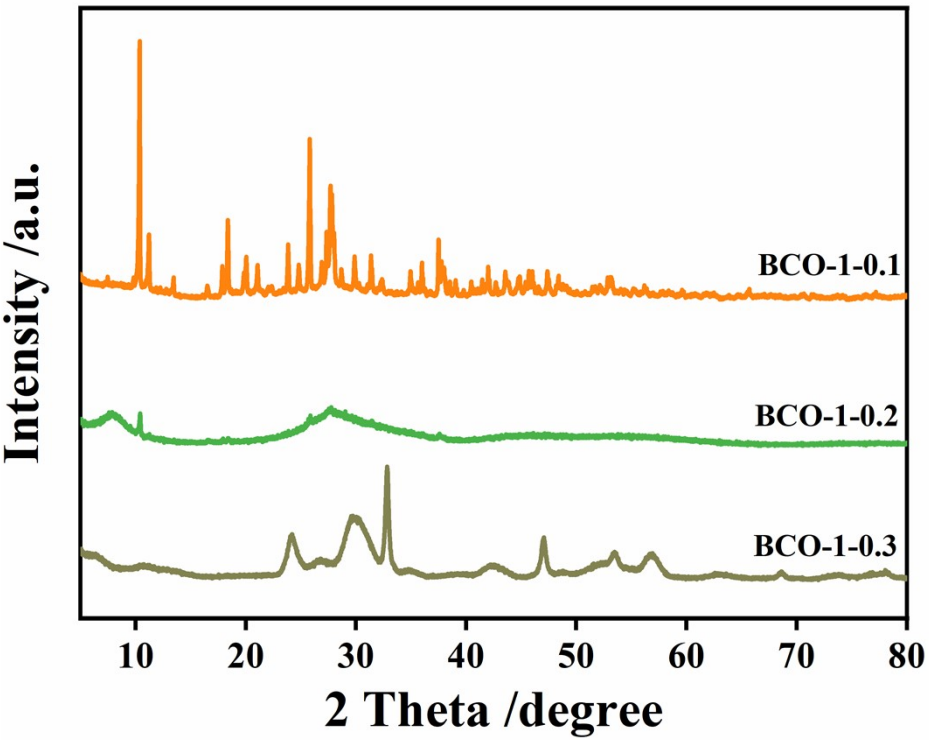

Figure S2. XRD patterns of different amounts of $KHCO_3$ treated samples.

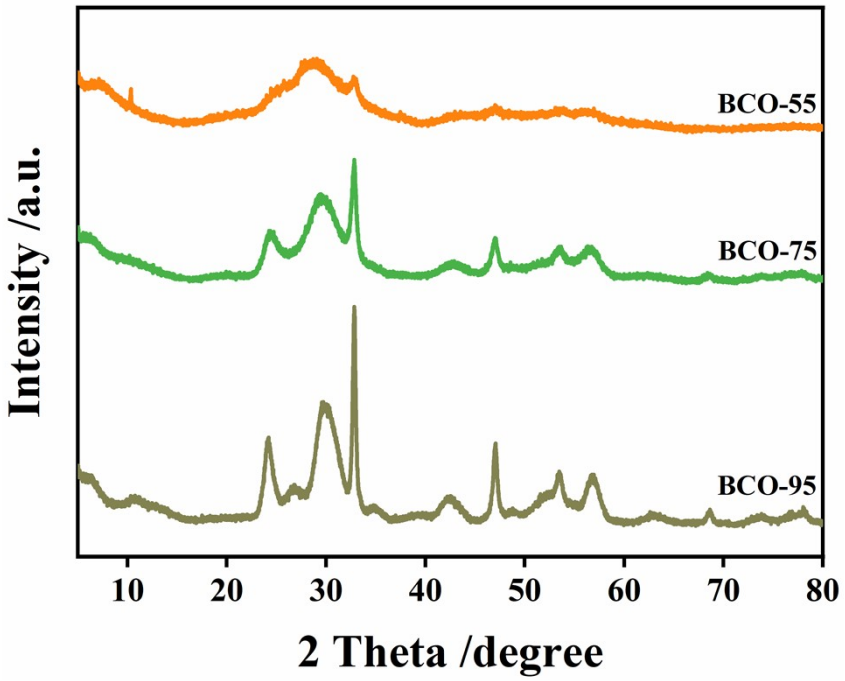

Figure S3. XRD patterns of samples obtained at different temperature in a water bath condition.

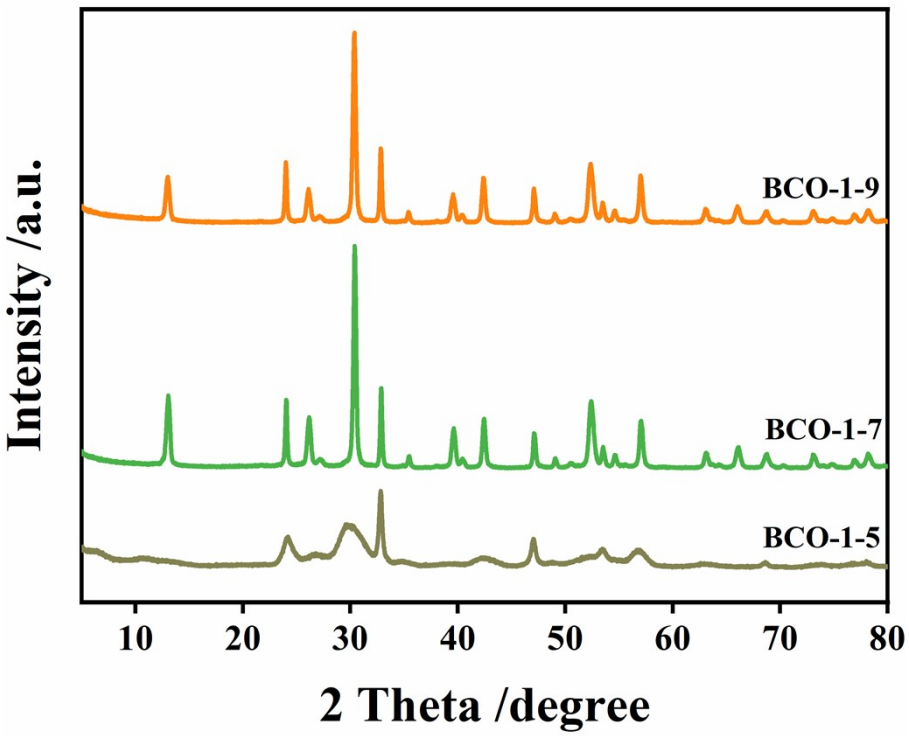

Figure S4. XRD patterns of samples obtained at different pH values at 95 °C water bath.

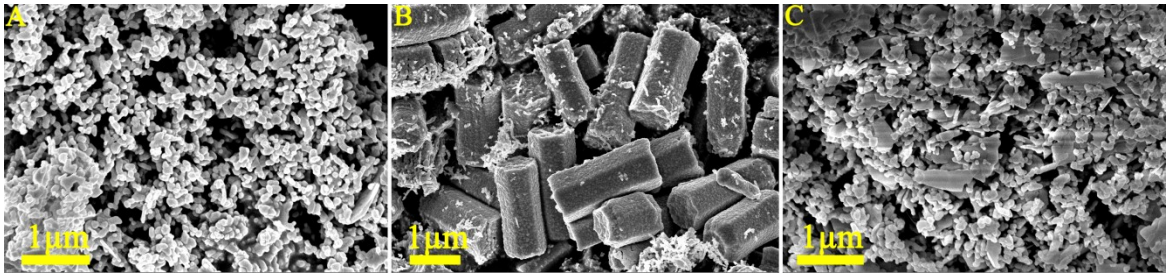

Figure S5. SEM images of samples obtained at pH values of 3 (A), 7 (B), and 9 (C) at 95 °C water bath .

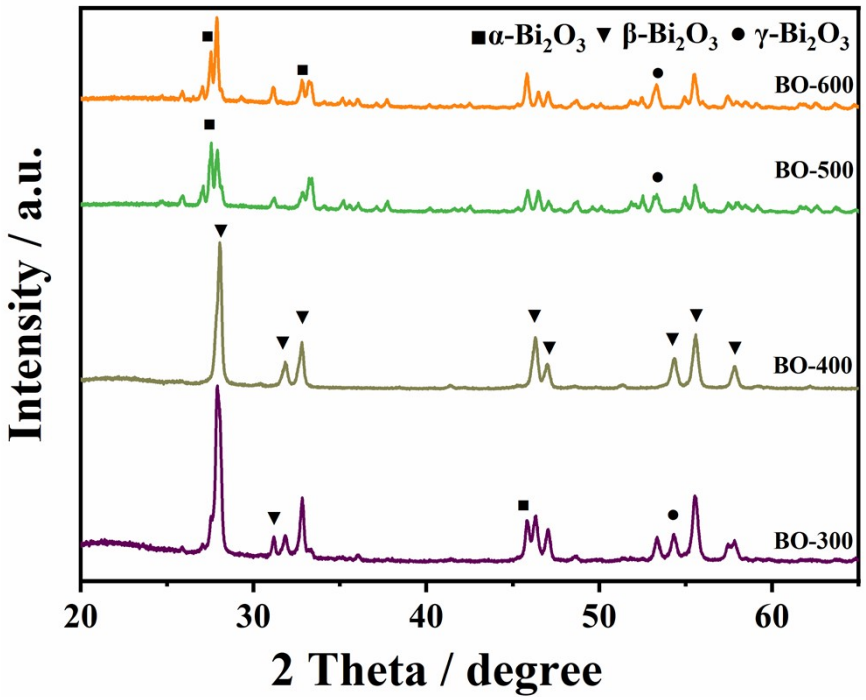

Figure S6. XRD patterns of the calcined BCO samples at different temperature.

Table S1. Surface area, total pore volume, and pore diameter of α-BO and β-BO microrods from N_2 adsorption-desorption.

Sample	Surface Area	Total pore volume	Pore Diameter Dv(d)
α-BO	70.3 m^2/g	6.164×10^{-2} cm^3/g	< 5 nm
β-BO	85.1 m^2/g	1.021×10^{-1} cm^3/g	< 5 nm

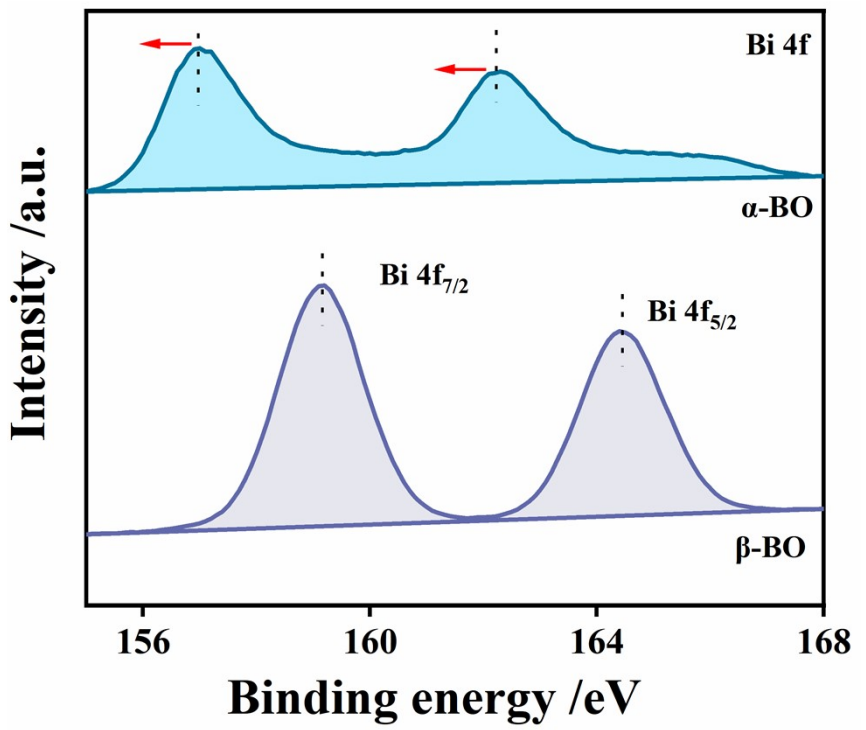

Figure S7 Bi4f XPS analysis of α-BO and β-BO.

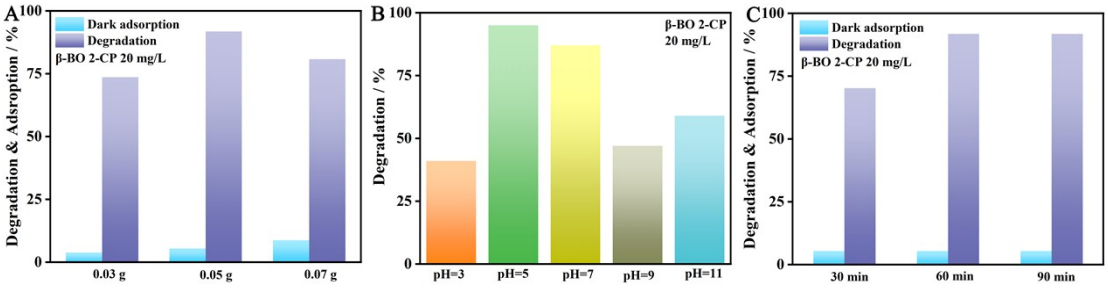

Figure S8. The influence of catalyst dosage (a), pH value (b), and reaction time (c) on degradation activities.

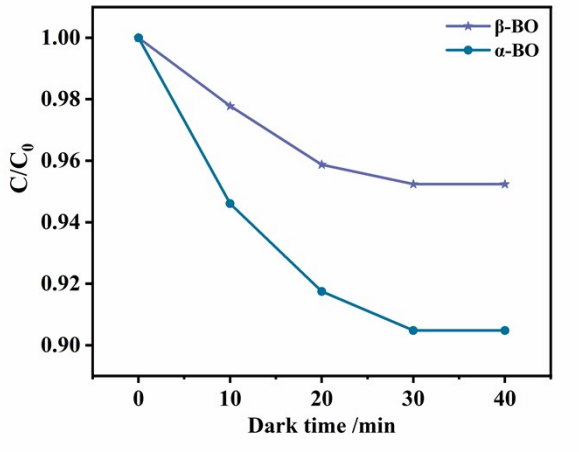

Figure S9. Time-dependent adsorption of 2-CP over α-BO and β-BO.

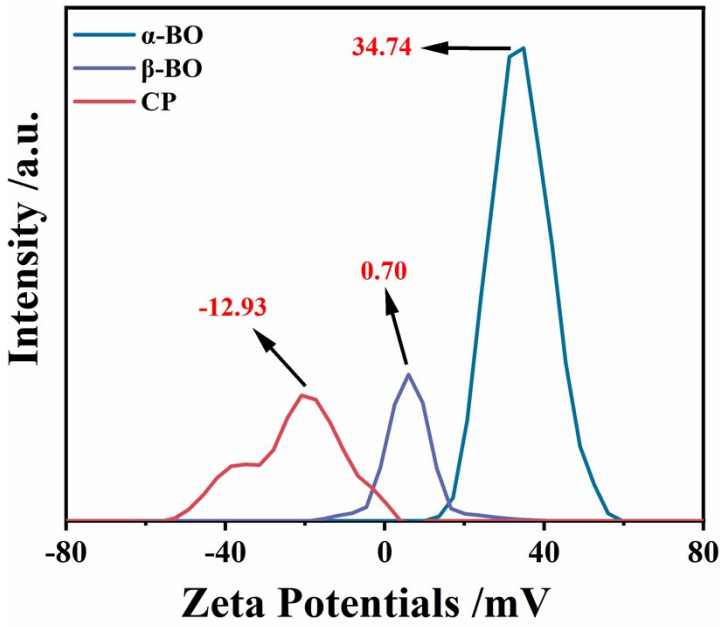

Figure S10. Zeta potentials of 2-CP, α-BO, and β-BO microrods.

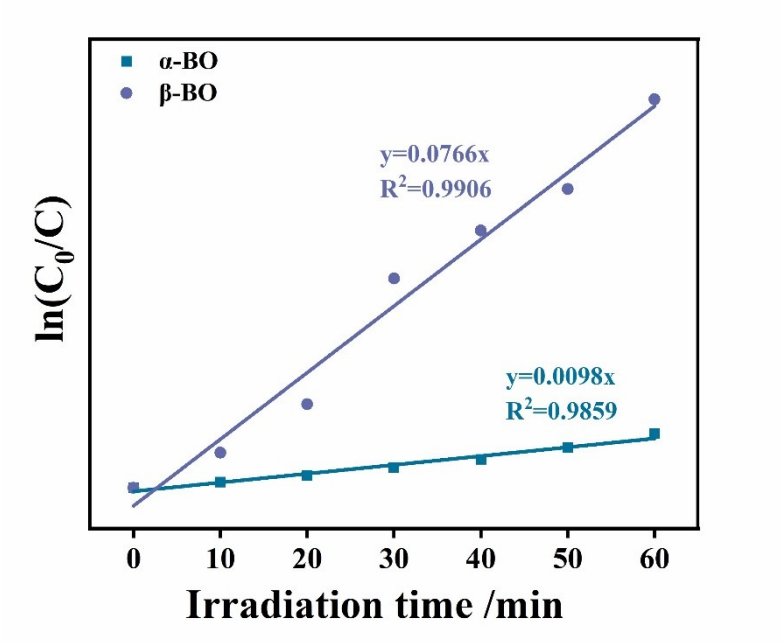

Fig. S11. First-order degradation kinetics (*k*) of α-BO and β-BO.

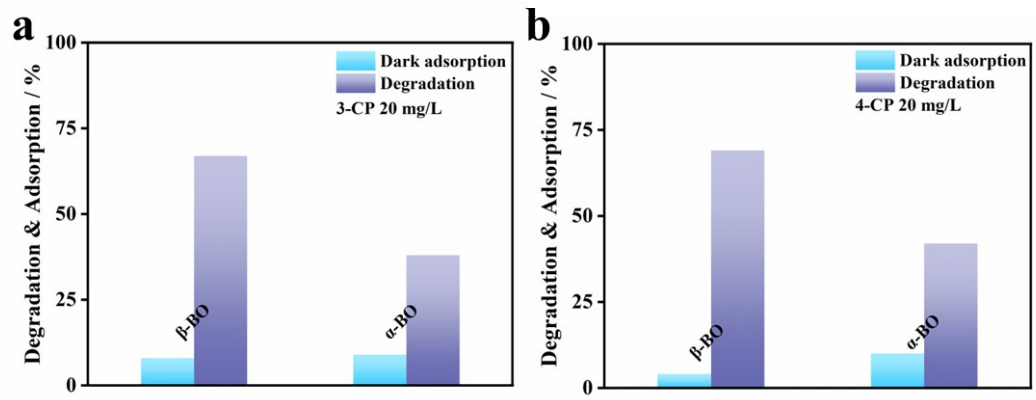

Figure S12. Visible-light activities of 3-CP (a) and 4-CP (b) degradation over α-BO and β-BO.

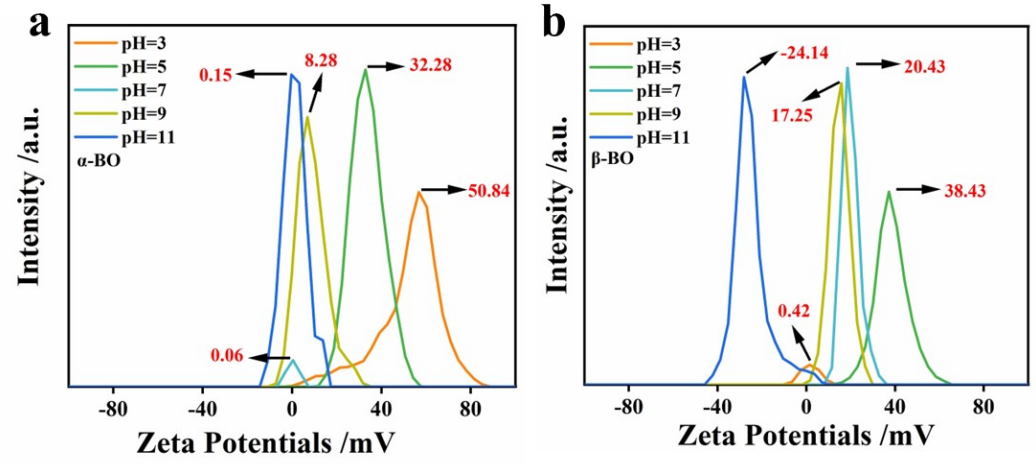

Figure S13. Zeta potentials of a-BO (a) and β-BO (b) at different pH.

Table S2. Comparison of photocatalytic 2-CP degradation with different published work.

Catalysts	Concentration mg/L	Reaction time/min	Degradation rate/%	References
BiO_{2-x}	20	90	75	Separation and Purification Technology, 2023, 316, 123792.
$Bi_2Fe_4O_9/BiFeO_3$	20	60	65	Applied Catalysis B: Environmental, 2022, 319, 121893.
g-C_3N_4/CdS	10	60	100	Applied Catalysis B: Environmental, 2023, 324, 122276.
Bi/Bi_2O_3/C	10	300	70	ACS Applied Nano Materials, 2019, 2, 2308.
β-Bi_2O_3	20	<60	100	This work